

# UC Berkeley

## UC Berkeley Previously Published Works

### Title

Cooling efficiency of a brushless direct current stand fan

### Permalink

<https://escholarship.org/uc/item/9qf8w0m4>

### Authors

Yang, Bin  
Schiavon, Stefano  
Sekhar, Chandra  
[et al.](#)

### Publication Date

2014-12-05

Peer reviewed

## Cooling efficiency of a brushless direct current stand fan

Bin Yang<sup>a, b, \*, 1</sup>, Stefano Schiavon<sup>c</sup>, Chandra Sekhar<sup>d</sup>, David Cheong<sup>d</sup>, Kwok Wai Tham<sup>d</sup>,  
William W Nazaroff<sup>e</sup>

<sup>a</sup> *Berkeley Education Alliance for Research in Singapore, 138602, Singapore*

<sup>b</sup> *School of Civil and Environmental Engineering, Nanyang Technological University, 639798, Singapore*

<sup>c</sup> *Center for the Built Environment, University of California, Berkeley, CA 94720, USA*

<sup>d</sup> *Department of Building, National University of Singapore, 117566, Singapore*

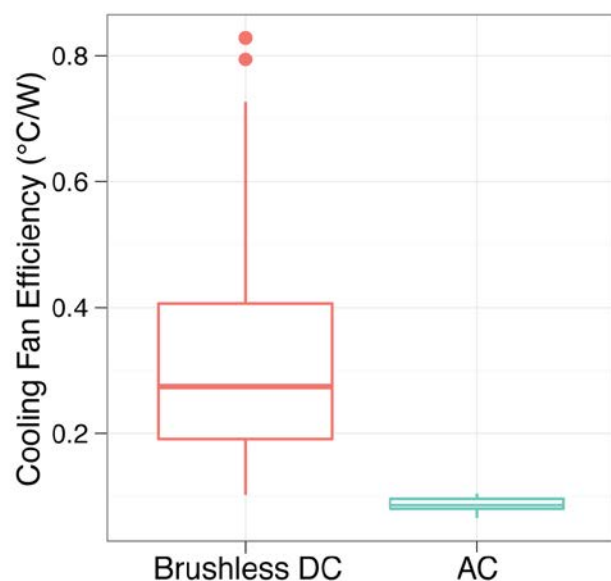
<sup>e</sup> *Department of Civil and Environmental Engineering, University of California, Berkeley, CA 94720, USA*

<sup>1</sup> *Current address: Department of Applied Physics and Electronics, Umeå University, Umeå, 90187, Sweden*

\*Corresponding author. Tel.: +46 90 7866117

E-mail address: bin.yang@umu.se (B. Yang).

### GRAPHICAL ABSTRACT



## HIGHLIGHTS

- Cooling fan efficiency (CFE) index quantifies fan performance.
- CFE index is influenced by temperature, fan speed setting, and fan-manikin distance.
- CFE has a non-monotonic relationship with fan speed.
- CFE index of a brushless DC fan is three times better than that of an AC fan.

## ABSTRACT

In warm environments, isothermal cooling by deliberately enhanced air movement can maintain thermal comfort using less energy than compressor-based air conditioning. To evaluate the performance of a brushless direct current (DC) stand fan, the cooling fan efficiency (CFE) index was measured in a climatic chamber under four dry-bulb temperatures (24, 26, 28, and 30 °C), six speed settings (corresponding to centreline speeds in the range 0.6-2.5 m/s at 1 m distance), two fan-manikin distances (1 and 2 m) and two orientations (front, side). The CFE index is defined as the ratio of the whole-body cooling effect generated by non-uniform airflow from the fan to its power consumption (°C/W). The CFE index overcomes the limitations of assessing the cooling effect based just on a few air speed measurements. The results show that the CFE index is influenced by dry-bulb temperature, fan speed setting, and fan-manikin distance, but not by fan-manikin orientation. The lower the temperature and the closer the fan, the higher is the CFE index. Increasing fan speed setting simultaneously enhances whole-body cooling and increases power use. Consequently, the CFE has a non-monotonic relationship with fan speed setting and the peak value is reached for an intermediate speed. As compared with previous testing results using an alternating current stand fan, the CFE index of the DC fan we tested is three times higher. As a complement to air-conditioning, the tested stand fan is a suitable energy-efficient technology for providing thermal comfort in warm environments.

*Keywords:* Cooling fan efficiency index; Thermal manikin; Equivalent temperature; Thermal comfort; Air movement

## **1. Introduction**

Elevated air speed is an effective method of cooling people in moderately warm indoor environments. An electrically powered mechanical fan can be used to enhance airspeed near people to cool them. Cooling fans can be used instead of, or to augment, compressor-based air-conditioning systems to contribute to occupant thermal comfort by means of isothermal cooling [1-3]. Furthermore, personal control over one's thermal environment can increase comfort, satisfaction and self-reported productivity [4-6]. Cooling fans are well-suited to provide personal control. Cooling the human body by means of elevated air movement under high dry-bulb temperature conditions contributes to substantial energy savings [7-9]. In cold environments, elevated air movement causes draft, defined as unwanted local cooling [10]. However, elevated air movement can enhance thermal comfort in warm environments [3, 11-19]. The use of fans for cooling may be more feasible in tropical than in temperate climates because tropically acclimatized people prefer slightly higher air movement and slightly cool thermal sensation [7, 20]. A comprehensive literature review on thermal comfort research conducted over the past twenty years has documented the theoretical and empirical support for using cooling fans [21]. Thermal comfort standards [22-24] allow for an increased indoor temperature to be offset by elevated air movement. Although perceived air quality is negatively affected by elevated temperature and relative humidity [25-26], perceived air quality is improved by elevated air speed [26-29].

Appearance, control options, and price are important parameters to be considered when purchasing cooling fans. However, little quantitative information is available regarding the cooling capacity and energy efficiency of fans. Comparing the performance of cooling fans from the point of view of cooling capacity and energy consumption is important for their application in practice, including their implementation as a means of providing thermal

comfort in an energy-efficient manner. To address this issue, Schiavon and Melikov [30] introduced the cooling fan efficiency (CFE) index, defined as the ratio between the fan-generated whole-body cooling effect (as measured with a thermal manikin) and fan power consumption. The CFE index allows one to objectively compare cooling fans in terms of their ability to cool people in an energy efficient manner. Schiavon and Melikov measured the CFE index for four fans (ceiling, desk, stand, and tower) in a real office at three dry-bulb temperatures and at different fan speed settings. The results revealed that the CFE index is sensitive enough to identify differences in the performance of the cooling devices and that the cooling fans generate a nonuniform velocity field around occupants, which cannot be described with a single airspeed. Schiavon and Melikov did not test either the effect of fan-manikin distance or the effect of fan-manikin orientation on the CFE index; therefore, the influence of these parameters on the CFE index is unknown. This knowledge gap is pertinent, because cooling fans that are under the direct control of people, such as desk fans and stand fans, can be used at different distances and with different orientations.

Fans that use brushless direct current (DC) motors are more energy-efficient than fans that use alternating current (AC) motors [31-33]. Motor operation depends on electromagnetic force, which is induced by rotor winding. Electromagnetic force has to be kept in the same direction. For AC motors, the direction of the stator's magnetic field is changed; for brushed DC motors, the current is reversed. In a brushed DC motor, a brush commutator is needed to reverse the current. In brushless DC motors, an electronic device, such as a semiconductor inverter, replaces the commutator. Brushless DC motors last longer, have low electromagnetic noise and are energy efficient. Brushless DC motors also can modulate speed easily and smoothly [33].

Most of the cooling fans available in today's markets use AC motors because the manufacturing cost is currently lower than for brushless DC motors. To focus on the potential

energy efficiency of fan-enhanced cooling, the present study evaluates a commercial cooling fan (Airmate S35113R) that employs a three-phase brushless DC motor. The fan has 24 speed settings and its peak power use is 17.3 W, which is less than half that of comparable AC fans. To our knowledge there have been no prior assessments of the cooling effect and the CFE index of brushless DC fans.

The aims of this research are to test the performance of a brushless DC fan utilizing the manikin-based equivalent temperature, fan power consumption and CFE index and to assess the effect of input parameters including fan-manikin distance and orientation on the CFE index. The CFE index for the brushless DC fan is quantitatively analysed and compared with values for the AC fans previously tested.

## **2. Methods**

### *2.1. Experimental facilities*

The experiments were carried out in the Field Environmental Chamber (FEC) at National University of Singapore (NUS). The dimensions of the FEC are  $11.0 \times 7.8 \times 2.6$  m (volume =  $223 \text{ m}^3$ ). It provides accurate control of dry-bulb temperature,  $t_a$  ( $\pm 0.5$  °C), and relative humidity, RH ( $\pm 3\%$ ). The FEC has an east-facing wall consisting of glass panels, which are attached with solar block film and equipped with internal blinds to reduce heat gain from solar radiation. The outdoor air temperature was between 31 °C and 32.5 °C during the period of study. Room air temperature was controlled by a variable air volume (VAV) air conditioning system. Relative humidity does not affect the thermal manikin measurements described below, and therefore it was not controlled, but it was continuously measured. One workstation was located at the centre of the chamber, which is far from the windows and supply air diffusers, so as to minimize their effect on measurements. Based on previous experiments performed in this room, the mean radiant temperature (MRT) could be assumed

equal to the dry-bulb temperature since the workstation is far from windows and there are no other significant radiant sources.

A three-phase brushless DC stand fan was used. The fan was situated in one of four positions: at 1 or 2 m distance (corresponding to 3 or 6 times the fan diameter) either in front of (zero degrees) or to the right of (ninety degrees) a dry-heat-loss thermal manikin. These distances and orientations were selected to correspond to common choices of users. The axis of the fan blades and motor are at 1.1 m height, equal to the breathing zone of a seated person. The fan consumes from 1.9 W (min speed) to 17.3 W (max speed), which generates airspeeds from 0.05 m/s to 2.5 m/s at 1 m distance and 0.05 m/s to 1.3 m/s at 2 m distance, respectively (Fig. 1). The detailed relationship between fan speed setting, fan power, and air speeds measured at 1.1 m height at the target location for the two tested distances (1 and 2 m) are reported in the Supplemental Information (Table A). Turbulence intensities varied between 19% and 27% with a median value of 24%. Air speeds and turbulence intensities at the target point (breathing area) were measured without the presence of the thermal manikin.

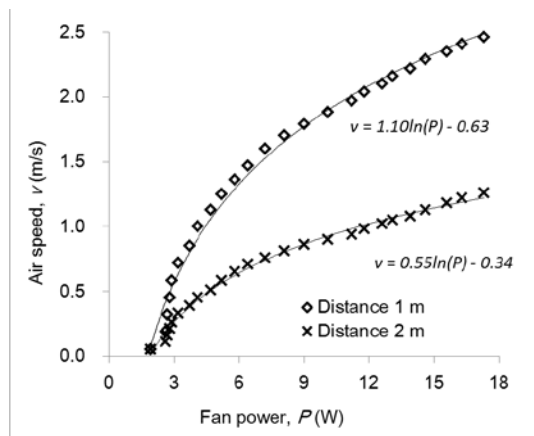


**Fig. 1.** Air speed ( $v$ ) measured at 1.1 m height at the target location as a function of fan power ( $P$ ) for the two tested distances between the fan and the target location (1 and 2 m).



**Fig. 2.** Experimental configuration for the case in which the fan was positioned 1 m in front of the thermal manikin.

## *2.2. Measuring instruments*

Dry-bulb temperature and RH were measured with TSI (Shoreview, MN, USA) indoor air quality meter model 7545, with 0-60 °C measuring range,  $\pm 0.4$  °C uncertainty for temperature, and 5-95% measuring range,  $\pm 3\%$  uncertainty for RH. Air speed was measured using Dantec (Skovlunde, Denmark) Dynamics' ComfortSense System, with a response time of 0.5 s and uncertainty of 0.01 m/s  $\pm 1\%$  of reading. Fan power was measured by Yokogawa (Tokyo, Japan) digital power meter model 2534 with 0-5 kW measuring range and 0.1 W uncertainty. Uncertainty for measured and derived quantities was assessed using standard methods [34, 35] and is reported in the Supplemental Information (Table B).

A dry-heat-loss thermal manikin, which simulates sensible heat loss from a human body, was used to evaluate the cooling effect of the fan. Latent heat losses are not included in this system. The manikin is shaped as an average-size Scandinavian woman, with a height of 1.68 m and total surface area of 1.48 m<sup>2</sup>. The manikin has 26 independently controlled body segments, comprising polystyrene shells wound with embedded nickel wire, serving to heat body parts and to monitor skin temperature. The manikin was calibrated before the experiments.

## *2.3. Experimental conditions*

Fan performance was measured at four dry-bulb temperatures (24, 26, 28, and 30 °C), six selected speed settings (4, 8, 12, 16, 20, and 24), two distances between the fan and thermal manikin (1 and 2 m) and two orientations (front and side). The experimental conditions are reported in Table 1. The 100 experiments (96 for all combinations plus 4 tests without the fan) were carried out in a random sequence. Measured dry-bulb temperatures were consistently within 0.3 °C of the set point for each experimental condition. The thermal manikin was



dressed with short-sleeved T-shirt, thin long trousers, underwear, socks and shoes (corresponding to approximately 0.45 clo), which represents conditions for a typical Singaporean office worker [36]. Its exposed body areas are face, neck, forearms and hands. The manikin was seated on a typical office chair (about 0.15 clo) as shown in Fig. 2.

**Table 1.** Tested conditions for various independent parameters.

Parameter	Level	Number of Cases
	24 °C	25
Dry-bulb temperature	26 °C	25
	28 °C	25
	30 °C	25
	0	4
	4	16
	8	16
Fan speed setting <sup>a</sup>	12	16
	16	16
	20	16
	24	16
Fan-manikin distance	1 m	48
	2 m	48
Fan-manikin orientation	Front	48
	Side	48

<sup>a</sup> When the fan speed setting was 0, measurements were done only one time for each of the tested dry-bulb temperatures. Table A in the Supplemental Information provides correlations between fan speed setting, fan power, and air speed at target distances.

#### 2.4. Experimental procedures

The manikin was operated in the “thermal comfort mode,” meaning that the surface temperature of the manikin was controlled to be the same as the skin temperature of an average person in a state of thermal comfort under the exposed environmental conditions [37-38]. The manikin’s surface temperature and power consumption were recorded for ten minutes after the steady-state condition was reached. In these experiments, steady state was defined as when the average surface temperature difference of the manikin during the preceding ten minutes changed by less than 0.05 °C [39]. Fan power consumption was recorded manually. The manikin was then removed, and air speeds and turbulence intensities were recorded four times in continuous three-minute intervals at each of four sampling heights (0.1, 0.6, 1.1 and 1.7 m). The four three-minute average values were used to calculate the final average value.

#### 2.5. Evaluating the CFE index

To quantify the cooling effect of the thermal environment with the fan, sensible heat loss measured from each body segment as well as from the whole manikin was transformed into a parameter named manikin-based equivalent temperature. The manikin-based equivalent temperature is defined as the temperature of a uniform enclosure in which a thermal manikin with realistic skin surface temperature would lose heat at the same rate as it would in the actual environment [40]. It is calculated as follows (Equation 1). The difference of manikin-based equivalent temperature with and without fan-generated airflow ( $\Delta t_{eq}$ ) calculated for each body segment and for the whole body was used to evaluate the fan cooling effect (Equation 2).

The CFE index ( $CFE$ , in °C/W) is defined as the ratio of the fan-generated whole-body cooling effect ( $\Delta t_{eq}$ , in °C) to the fan power consumption ( $P$ , in W) [30] (Equation 3). The

CFE index does not address the thermally asymmetric cooling effect for different body segments and it only considers the whole-body cooling effect.

$$t_{eq} = t_{sk} - \frac{Q_t}{h_{cal}} \quad (1)$$

where  $t_{eq}$  = manikin-based equivalent temperature [ $^{\circ}\text{C}$ ],  $t_{sk}$  = skin temperature [ $^{\circ}\text{C}$ ],  $Q_t$  = sensible heat loss [ $\text{W}/\text{m}^2$ ], and  $h_{cal}$  = dry heat transfer coefficient [ $\text{W}/\text{m}^2$  per  $^{\circ}\text{C}$ ].

$$\Delta t_{eq} = t_{eq, fan} - t_{eq, no fan} \quad (2)$$

where  $\Delta t_{eq}$  = manikin-based equivalent temperature difference [ $^{\circ}\text{C}$ ],  $t_{eq, fan}$  = manikin-based equivalent temperature with the fan [ $^{\circ}\text{C}$ ],  $t_{eq, no fan}$  = manikin-based equivalent temperature without the fan [ $^{\circ}\text{C}$ ].

$$CFE = (-1) \frac{\Delta t_{eq}}{P} \quad (3)$$

## 2.6. Statistical analysis

The distributions of measured whole-body cooling effect and the CFE index are presented as box-plots. The line inside the box, the bottom line, and the top line show the median, 25<sup>th</sup> percentile, and 75<sup>th</sup> percentile, respectively. The end of each whisker line shows the lesser extremum of the maximum (minimum) or the median plus (minus) 1.5 times the interquartile range. Measured results beyond the end of a whisker are plotted as circles. For results that are empirically determined to be normally distributed, we report the mean and standard deviation (e.g. mean (SD)); results that are not normally distributed are described with median and first and third quartile in parenthesis (e.g. median (first quartile, third quartile)). Distributions were tested for normality using the Shapiro-Wilk normality test. To assess the influence of independent variables on the outcome measures, the ANOVA test was used. Results were assumed to attain statistical significance when  $p < 0.05$ . The statistical analysis was performed with R version 2.15.1. Graphs were developed using GGplot2.

### 3. Results

#### 3.1. Cooling effect and Cooling Fan Efficiency (CFE) index

The whole-body cooling effect ( $\Delta t_{eq}$ ) and the CFE index were determined for each experimental condition studied. The results in tabular format are reported in Table C (see Supplemental Information). Considering all tests, the median value for  $\Delta t_{eq}$  is  $-2.4$  °C (first quartile =  $-3.7$  °C, third quartile =  $-1.5$  °C),  $P$  is  $9.2$  W ( $4.7$  W,  $13.9$  W), and the CFE index is  $0.27$  °C/W ( $0.19$  °C/W,  $0.41$  °C/W), respectively.

##### 3.1.1 Cooling effect

###### 3.1.1.1 Whole-body cooling effect

In Fig. 3, box-plots of whole-body cooling effect are reported in relation to dry-bulb temperature, fan speed setting, fan-manikin distance, and fan-manikin orientation. The whole-body cooling effect for this set of experimental conditions does not exhibit a normal distribution ( $W = 0.93$ ,  $p < 0.001$ ). One-way ANOVA tests show that dry-bulb temperature, fan speed setting and fan-manikin distance each have statistically significant influence on the whole body cooling effect ( $p < 0.001$ ); fan-manikin orientation did not have a statistically significant influence.

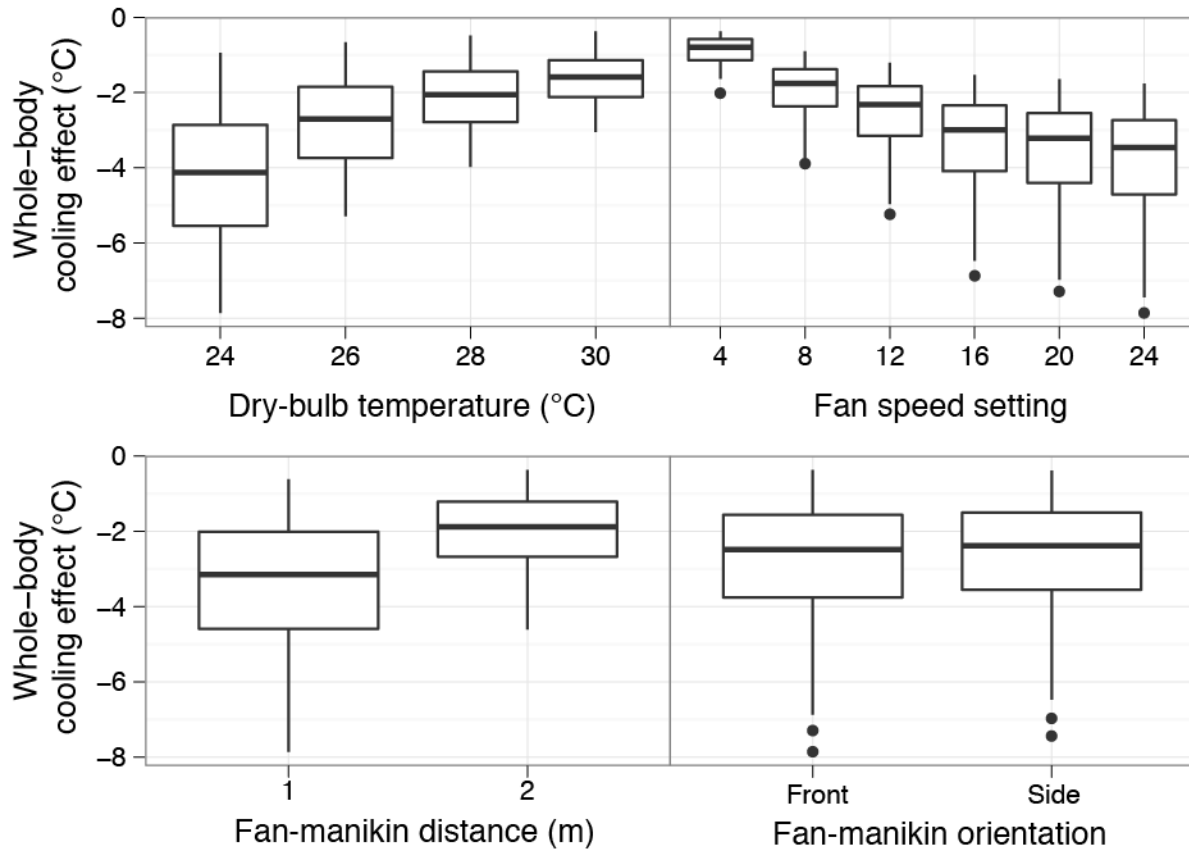


**Fig. 3.** Effect of dry-bulb temperature, fan speed setting, fan-manikin distance and fan-manikin orientation on whole-body cooling effect ( $\Delta t_{eq}$ ).

As anticipated, the influence of dry-bulb temperature on the whole-body cooling effect is strong. When the dry-bulb temperature is 24 °C, the median whole-body cooling effect across all test conditions is -4.1 °C (-5.5 °C, -2.9 °C). When the air temperature is increased to 30 °C,  $\Delta t_{eq}$  decreases to -1.6 °C (-2.1 °C, -1.1 °C). The medians change from -4.1 to -2.7 °C and from -2.1 to -1.6 °C when air temperature changes from 24 °C to 26 °C and from 28 °C to 30 °C, respectively. Hence, as expected, the effect of temperature change on the whole-body cooling effect diminishes as the air temperature approaches the skin temperature. It is important to stress that we used a dry-heat-loss thermal manikin in these experiments; thus, latent losses were not measured. For a real person, with the increase of air temperature, there

would be an increase of perspiration that would provide some additional cooling to an extent that would be influenced by the absolute humidity of room air.

The influence of fan speed setting on the whole-body cooling effect is also strong. When fan speed setting is 4 (corresponding to  $P = 2.9$  W),  $\Delta t_{eq}$  is  $-0.8$  °C ( $-1.1$  °C,  $-0.6$  °C). When fan speed setting is increased to the maximum level of 24 ( $P = 17.3$  W),  $\Delta t_{eq}$  increases to  $-3.5$  °C ( $-4.7$  °C,  $-2.7$  °C). The medians change from  $-0.8$  to  $-1.8$  °C, from  $-2.3$  to  $-3.0$  °C and from  $-3.2$  to  $-3.5$  °C, respectively, when the fan speed setting is changed from 4 to 8 (2.9 to 4.7 W), from 12 to 16 (7.2 to 11.2 W), and from 20 to 24 (13.9 to 17.3 W).

Since the fan is designed for personal use, we have chosen short distances between the fan and manikin for testing. When the fan-manikin distance is 1 m,  $\Delta t_{eq}$  is  $-3.2$  °C ( $-4.6$  °C,  $-2.0$  °C) for the tested cases. When the distance is increased to 2 m,  $\Delta t_{eq}$  declines to  $-1.9$  °C ( $-2.7$  °C,  $-1.2$  °C). Thus, as expected, the smaller fan-manikin distance is associated with a higher whole-body cooling effect.

Fan performance was tested for two different fan-manikin orientations. When fan is positioned in front of the manikin,  $\Delta t_{eq}$  is  $-2.5$  °C ( $-3.8$  °C,  $-1.6$  °C). When fan is located at the side,  $\Delta t_{eq}$  is  $-2.4$  °C ( $-3.6$  °C,  $-1.5$  °C). Hence, the effect of orientation on the whole-body cooling effect is negligible ( $p = 0.78$ ). For practical purposes, a cooling fan can be located at a person's side if it is difficult to find a suitable place to position the fan in front of the subject because of a desk or partition. Asymmetric exposure and local cooling effects for upwind and downwind body segments are discussed in the next section.

In summary, one can conclude that dry-bulb temperature, fan speed setting, and fan-manikin distance each influence the whole-body cooling effect of the tested fan. However, the cooling effect is not influenced by fan-manikin orientation.

### 3.1.1.2. Local cooling effect

The local cooling effect ( $\Delta t_{eq, local}$ ) for each body segment depends on local airflow, clothing level, body segment area, and dry-bulb temperature. The values of  $\Delta t_{eq, local}$  obtained at the lowest dry-bulb temperature (24 °C), highest fan speed setting (24,  $P = 17.3$  W), at 1 m distance, and for the two fan-manikin orientations, are shown in Fig. 4. The interaction of the fan-generated airflow with the manikin's generated thermal plume has direct influence on the local cooling effect. As expected, the results indicate that the head region of the manikin (skull, left/right face, back of the neck) is the area most cooled by fan-generated airflow. The local cooling effect for the left and right chest is comparable to or even slightly stronger than the facial cooling effect, which may be a consequence of additional airflow deflected by the table. Apart from the head and chest regions, cooling is evident for the arm and thigh regions, demonstrating the wide coverage provided by the stand fan. The tested fan can cool more body segments effectively as compared with the spot cooling that is typically generated by personalized ventilation air terminal devices [41-42].

Local cooling for front and side fan-manikin orientations can be compared. Since the fan is located at the right side of the manikin during the side orientation, the left side of the body is in the wake region of fan-generated airflow. The weakened cooling effect is seen especially for left side of the face and chest. For the right side of the back and also the back of the neck, the local cooling effects are enhanced by windward exposure. There is no clear influence of these local conditions on the whole-body cooling effect.

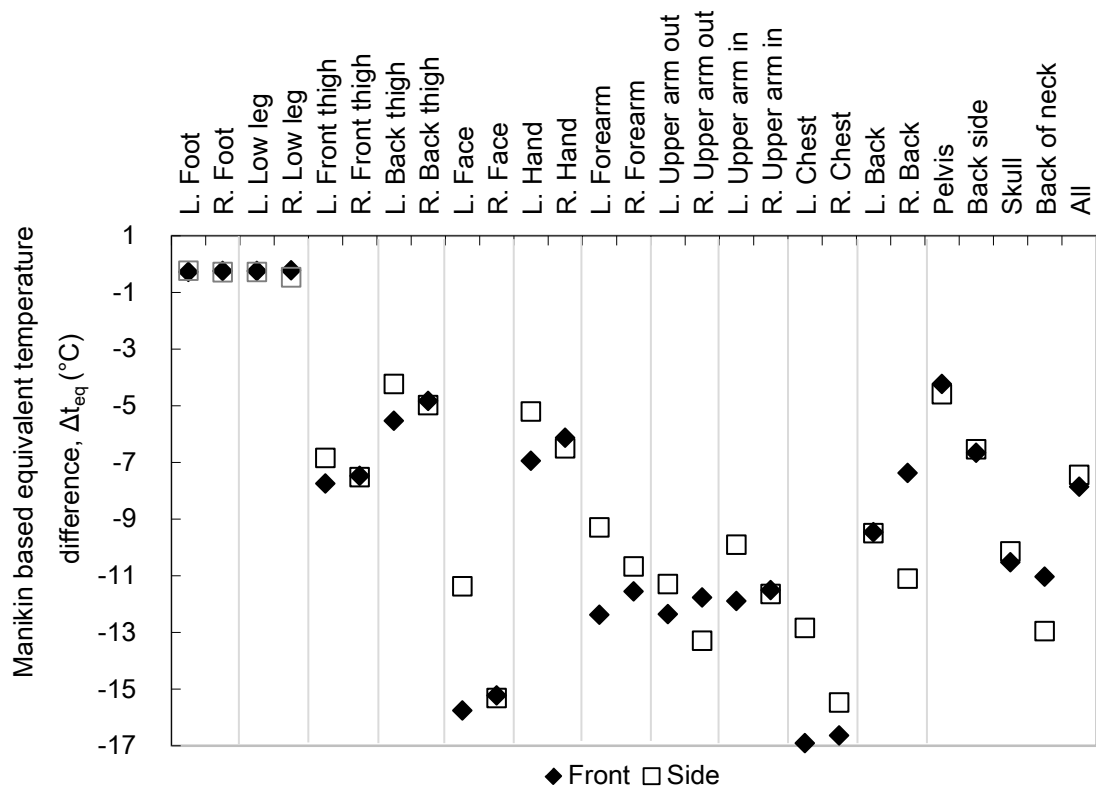


**Fig. 4.** Cooling effect comparison between front and side fan-manikin orientations for 24 °C dry-bulb temperature, fan speed setting of 24 ( $P = 17.3$  W) and 1 m fan-manikin distance.

### 3.1.2. Cooling Fan Efficiency (CFE) index

Fig. 5 displays the effect of dry-bulb temperature, fan speed setting, fan-manikin distance, and fan orientation on the CFE index. One-way ANOVA tests show that dry-bulb temperature, fan speed setting and fan-manikin distance are each statistically significant factors influencing the CFE index ( $p < 0.01$ ). However, fan orientation does not affect the CFE index value.



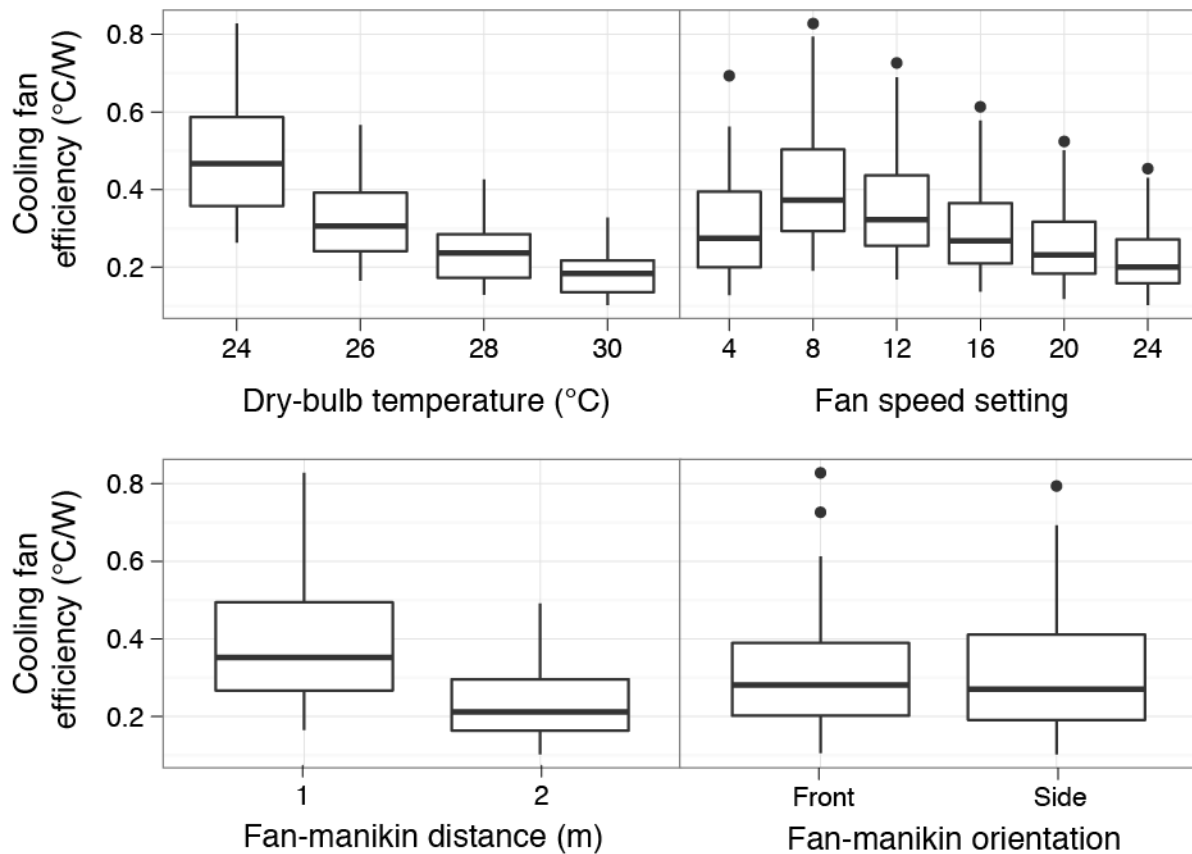


**Fig. 5.** Effect of dry-bulb temperature, fan speed setting, fan-manikin distance and fan-manikin orientation on the cooling fan efficiency index.

The influence of dry-bulb temperature on the CFE index is strong. For an air temperature of 24 °C, the median CFE index is 0.47 °C/W (0.36 °C/W, 0.59 °C/W). When the air temperature is increased to 30 °C, the median CFE index decreases to 0.18 °C/W (0.14 °C/W, 0.22 °C/W). The median CFE values change across a larger range (from 0.47 to 0.31 °C/W) when air temperature changes from 24 to 26 °C as compared to when air temperature changes from 28 to 30 °C, for which the median CFE index changes from 0.24 to 0.18 °C/W.

The influence of fan speed setting on the CFE index is also strong. When the fan speed setting is 8 ( $P = 4.7$  W), the CFE index reaches its maximum value: 0.37 °C/W (0.29 °C/W, 0.50 °C/W). The median value declines to 0.27 °C/W for a fan speed setting of 4 ( $P = 2.9$  W)

and to 0.20 °C/W for a fan speed setting of 24 ( $P = 17.3$  W). Increasing the fan speed setting simultaneously enhances the whole-body cooling effect and the power use.

It is noteworthy that the CFE index exhibits a non-monotonic relationship with fan speed setting, with a peak value attained at an intermediate speed. To understand this feature, it is necessary to consider how the cooling effect and fan power are affected by air speed (in this case measured at 1.1 m height). Our data show that the whole-body cooling effect has an approximate linear relationship with fan air speed (Equation 4).

$$|CE| = c_1 v \quad (4)$$

where  $|CE|$  = absolute value of cooling effect [°C],  $c_1$  = constant [°C s/m], and  $v$  = target air speed measured at 1.1 m height [m/s]. The constant,  $c_1$ , varies primarily with the dry-bulb temperature. Cooling effect versus target air speed for 1 m fan-manikin distance and front fan-manikin orientation is shown in Fig. 6 as an example. All results for different fan-manikin distances and orientations are shown in the Supplemental Information (Figs. A1-A4).

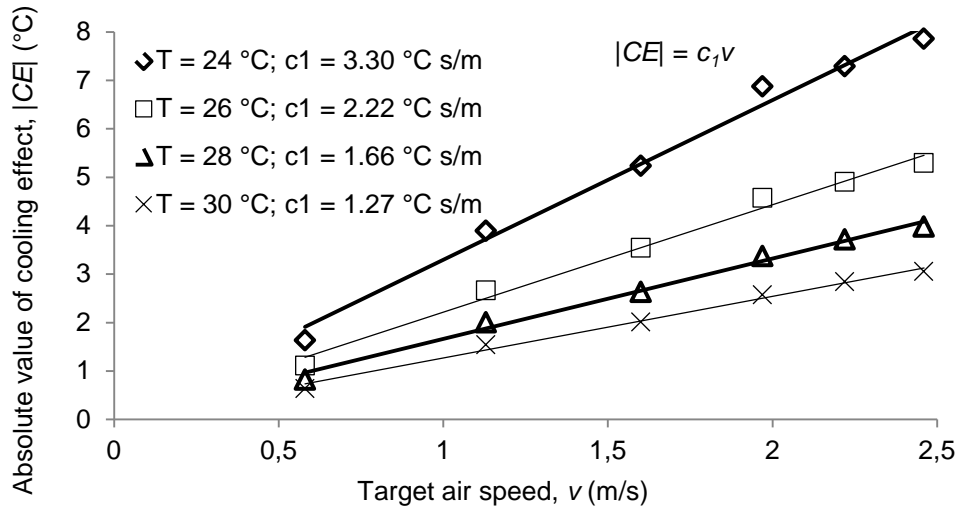


**Fig. 6.** Cooling effect versus target air speed for 1 m fan-manikin distance and front fan-manikin orientation. (The parameter  $c_1$  in the legend is the same as  $c_1$  in equation (4).)

To consider the influence of the dry-bulb temperature and the target air speed together, another equation with lumped parameters is used (Equation 5), which shows that cooling effect is proportional to target air speed and temperature difference between skin temperature and dry-bulb temperature.

$$|CE| = c^*(T^* - T)v \quad (5)$$

where  $c^*$  = constant [s/m],  $T^*$  = reference temperature, approximately equal to the skin temperature [°C] and  $T$  = dry-bulb temperature [°C]. The cooling effects versus the product of a temperature difference and target air speed for different fan-manikin distances and fan-manikin orientations are shown in the Supplemental Information (Figs. B1-B4). The reference temperature is chosen to obtain the best fit of the regression equation (i.e., the highest  $R^2$ ). The parameters  $c^*$  and  $T^*$ , and the corresponding value of  $R^2$ , for different fan-manikin distances and fan-manikin orientations are shown in Table D in the Supplemental Information.

Fan power varies approximately with the cube of the target air speed (Equation 6).

$$P = c_2v^3 + c_3 \quad (6)$$

where  $P$  = fan power [W],  $c_2$  = constant [ $\text{W s}^3/\text{m}^3$ ] and  $c_3$  = constant [W]. The two constants depend on the fan-manikin distance. The relationship between fan power and target air speed for 1 m fan-manikin distance is shown in Fig. 7. All results for different fan-manikin distances are shown in the Supplemental Information (Figs. C1-C2).

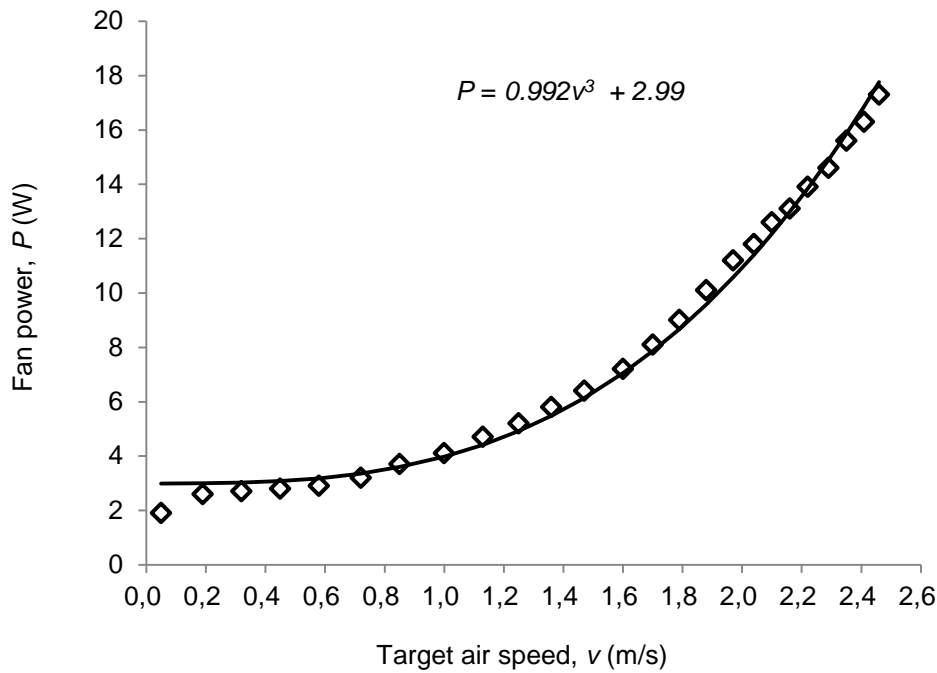


**Fig. 7.** Fan power versus target air speed for 1 m fan-manikin distance.

The CFE index is obtained as the ratio of Equation 4 to Equation 6 as shown in Equation 7.

$$CFE = \frac{c_1 v}{c_2 v^3 + c_3} \quad (7)$$

The CFE exhibits non-monotonic behaviour, which may be deduced by interpreting Equation 7 in the limits of small and large air speeds. For sufficiently small airspeed, the denominator is dominated by the constant term, and the CFE index varies in proportion to airspeed. Conversely, for sufficiently large airspeed, the denominator is dominated by the cubic airspeed term. In this limit, the CFE index varies in inverse proportion to airspeed squared. Given these behaviours at high and low airspeeds, and since CFE is a continuous function of  $v$ , its maximum value must lie between the limits of low and high airspeed. Empirically, at the level of granularity tested in this study, we found that for any particular combination of dry-bulb temperature, fan-manikin distance, and orientation, the maximum

CFE index occurred at a fan-speed setting of 8 ( $P = 4.7 \text{ W}$ ), which corresponds to airspeeds of 1.1 m/s and 0.5 m/s at fan-manikin distances of 1 m and 2 m, respectively. At this fan-speed setting, across the range of other conditions tested, the median CFE index was  $0.38 \text{ }^\circ\text{C/W}$  ( $0.26 \text{ }^\circ\text{C/W}$ ,  $0.54 \text{ }^\circ\text{C/W}$ ).

At a fan-manikin distance of 1 m, the median CFE index was  $0.35 \text{ }^\circ\text{C/W}$  ( $0.27 \text{ }^\circ\text{C/W}$ ,  $0.49 \text{ }^\circ\text{C/W}$ ). At a fan-manikin distance of 2 m, the median CFE index was  $0.21 \text{ }^\circ\text{C/W}$  ( $0.16 \text{ }^\circ\text{C/W}$ ,  $0.30 \text{ }^\circ\text{C/W}$ ). When fan was situated in front of the manikin, the median CFE index was  $0.28 \text{ }^\circ\text{C/W}$  ( $0.20 \text{ }^\circ\text{C/W}$ ,  $0.39 \text{ }^\circ\text{C/W}$ ). When fan is positioned at the side of the manikin, the median CFE index was statistically unchanged:  $0.27 \text{ }^\circ\text{C/W}$  ( $0.19 \text{ }^\circ\text{C/W}$ ,  $0.41 \text{ }^\circ\text{C}$ ). The CFE index does not address thermally asymmetric cooling effects for different body segments.

One expects that the typical distance between a stand fan and a person being cooled would be less than 2 m. As illustrated by Fig. 5, and consistent with expectations, it is more energy efficient to locate the fan closer to a person rather than farther (i.e., at 1 m instead of 2 m).

The orientation of the fan relative to the manikin did not affect the CFE index; however, the side orientation did create asymmetric local cooling. To the authors' knowledge, field data are not available to show whether asymmetric local cooling effects, as determined with a thermal manikin, influence human thermal acceptability in practice. Laboratory studies with human subjects have indicated that such asymmetry may not be a problem [15, 29]. For example, Arens et al. showed in a laboratory study that involved 3.5-h exposures and 119 subjects that people were not bothered by asymmetry if they also expressed the desire to not change the amount of air movement. Only if the airflow rate were too high would dissatisfaction be attributed to thermal asymmetry [15].

### *3.2. Vertical distribution of air speed*

The vertical distributions of air speeds, as measured at 0.1, 0.6, 1.1, and 1.7 m height above the floor, are depicted in Fig. 8. Higher air movement is generated for upper body parts,

especially near the head of the seated person, since the centre of fan blades is at 1.1 m height. Maximum air speeds (2.5 m/s for 1 m distance and 1.3 m/s for 2 m distance) were recorded at the 1.1 m height. Some of the air speed values are above the limits suggested by thermal comfort standards, 0.8 m/s and 1.2 m/s, respectively, for people without and with personal control over air speed [22]. Those upper limits have been questioned and higher limits have been suggested [15-16, 18, 20, 43]. Even if higher values have been proposed, it is possible that 2.5 m/s could be unacceptable due to the risk of lifting papers on a desk. According to a survey of 1538 people in China, 87% of respondents mentioned the risk of lifting papers as a main disadvantage of using fans [43]. It is noteworthy that at the fan speed setting of 8 ( $P = 4.7$  W), at which the highest CFE index values were obtained, the peak air speed at 1 m distance was 1.1 m/s, below the upper airspeed limit indicated by thermal comfort standards.

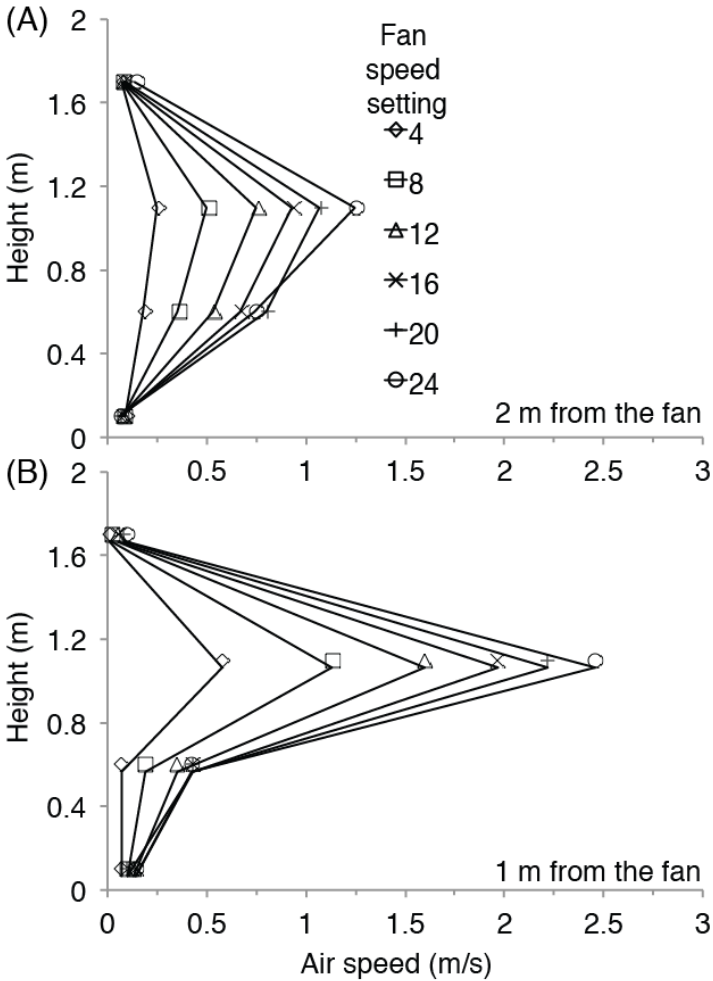


**Fig. 8.** Air speed measured at 0.1, 0.6, 1.1, and 1.7 m height above floor without the manikin for (A) 2 m distance and (B) 1 m distance between the fan and the measuring line. The fan's axis of rotation was at a height of 1.1 m. Air speeds were measured along a vertical line directly downwind of the fan.

### *3.3. Other influencing factors for CFE*

The CFE index was measured in this study in relation to dry-bulb temperatures, fan speed settings, and fan-manikin distances. However, clothing thermal insulation and its distribution over the manikin's body, the chair's thermal insulation, the manikin's emulated metabolic rate, the manikin body posture, furniture location and room boundary conditions, among other factors, may also influence the CFE index values. The influence of these parameters was not assessed in the present study. Furthermore, this study used a dry-heat-loss manikin to quantify the cooling effect for fan-generated air movement in an environment with uncontrolled RH. The degree to which these results inform fan-enhanced cooling for human subjects is limited by the lack of evaporative heat loss associated with perspiration in these experiments. In our view, in light of the limited available information about latent cooling from humans under the conditions tested, it is better for us to report accurately what our experiments did measure and to note clearly the exclusion of latent heat transfer as a limitation to be addressed in future studies. Schiavon and Melikov [30] have discussed the relationships between the manikin-determined CFE index and the thermal comfort of human subjects. Apart from pursuing high values of the CFE index, several practical factors including position of fan, indoor aesthetics, noise control, avoidance of paper blowing, and avoidance of non-thermal discomfort must also be considered. A standard method for evaluating a more comprehensive set of performance indices would be beneficial for fan designers, manufacturers and users.

### 3.4. Comparison with previous tested fan

The CFE index values obtained in these tests are considerably higher ( $p < 0.001$ ) than those previously reported for a geometrically similar stand fan driven by an AC motor [30]. Fig. 9 illustrates the comparison between brushless DC fan studied here and AC stand fans previously investigated. The median CFE for the brushless DC fan is  $0.27\text{ }^{\circ}\text{C}/\text{W}$  ( $N = 96$ ), more than three times larger than the corresponding value for the AC fan,  $0.086\text{ }^{\circ}\text{C}/\text{W}$  ( $N = 5$ ). Hence, the AC fan, for comparable cooling effects, has much higher power requirements. Part of the advantage of the tested fan can be attributed to the use of a brushless DC motor instead of an AC motor. Other reasons could be related to the design of the fan blades and differences in test conditions. Dry-bulb temperature clearly has a significant effect of the whole-body cooling effect and on the CFE index. The earlier stand fan was tested under similar dry-bulb temperature conditions as these experiments at  $25, 27$  and  $30\text{ }^{\circ}\text{C}$ . Our findings about the energy benefits of the brushless DC motor align with results from previous studies [31-32].

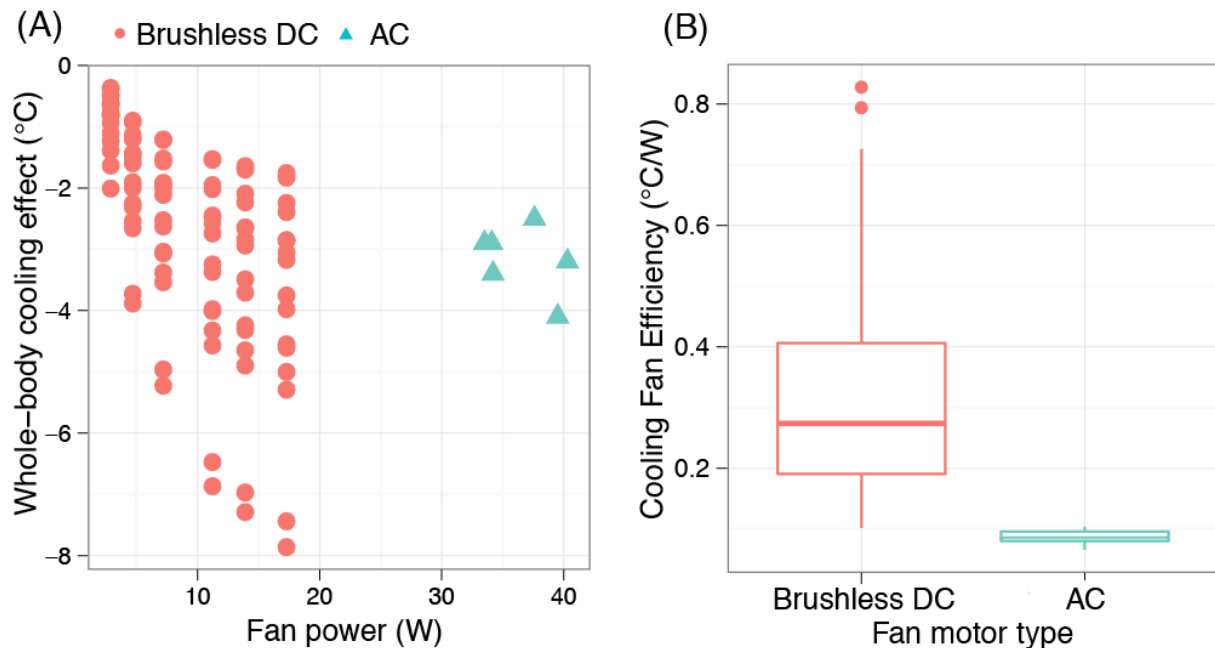




**Fig. 9.** Comparison between the newly collected data for a brushless DC stand fan and the data from Schiavon and Melikov [30] for an AC stand fan. (A) Comparison between the cooling effect and the fan power. (B) Cooling fan efficiency (CFE) index for the two fans.

#### **4. Assessing the cooling effect**

##### *4.1 Traditional standard effective temperature method for assessing the cooling effect*

Thermal comfort standards propose calculation methods, based on the standard effective temperature (SET\*), to predict the cooling effect of elevated air speed for improving thermal comfort in warm environments [22-23]. Schiavon et al. [44] described how the standard effective temperature has been implemented in ASHRAE Standard 55-2013 and how the cooling effect is calculated. SET\* is defined as the equivalent air temperature of an isothermal environment, at a relative humidity of 50%, in which a subject, wearing clothing standardized for the activity concerned, has the same heat stress and thermoregulatory strain as in the actual environment [45]. The cooling effect of air movement is calculated assuming that the body is exposed to a uniform airflow field, i.e. the same velocity is experienced by each body part [46]. However, this assumption is not directly applicable to cooling fans as they generate nonuniform airflow fields. ASHRAE Standard 55-2013 requires use of the average velocity (e.g., the average among air speeds measured at 0.1, 0.6 and 1.1 m for a seated occupant). In the research community, the use of maximum velocity instead of average velocity has been discussed. In this study, data collected in the experiments with a stand fan and a thermal manikin are used to test and compare these two calculation methods.

Cooling effects, calculated according to ASHRAE Standard 55-2013 based on maximum speed and average speed, are compared with the measured results in Fig. 10 (see also Table E in the Supplemental Information). To calculate the cooling effect, the following parameters were used: dry bulb temperature (equal to the mean radiant temperature) = 26 °C; RH = 55%; clothing insulation level = 0.6 clo (human clothing plus office chair); metabolic activity level

= 1.1 met. The air speeds measured at 2 m from the fan were used. The cooling effect calculations were performed with the CBE Thermal Comfort Tool for ASHRAE Standard 55 [47]. Fig. 10 shows substantial differences in the inferred cooling effect assessed by the manikin and using the method presented in ASHRAE Standard 55. The selection of air speed (average or maximum) has a strong influence on the cooling effect calculations. As expected, the cooling effect of the manikin is lower than that based on the SET\* calculations, because the thermal manikin does not incorporate evaporative heat loss. However, notwithstanding this methodological inconsistency, the difference is surprisingly large. In searching for an explanation, we became aware of a possible issue in the existing standard and we developed an updated calculation method that is potentially better than the method in the standard.

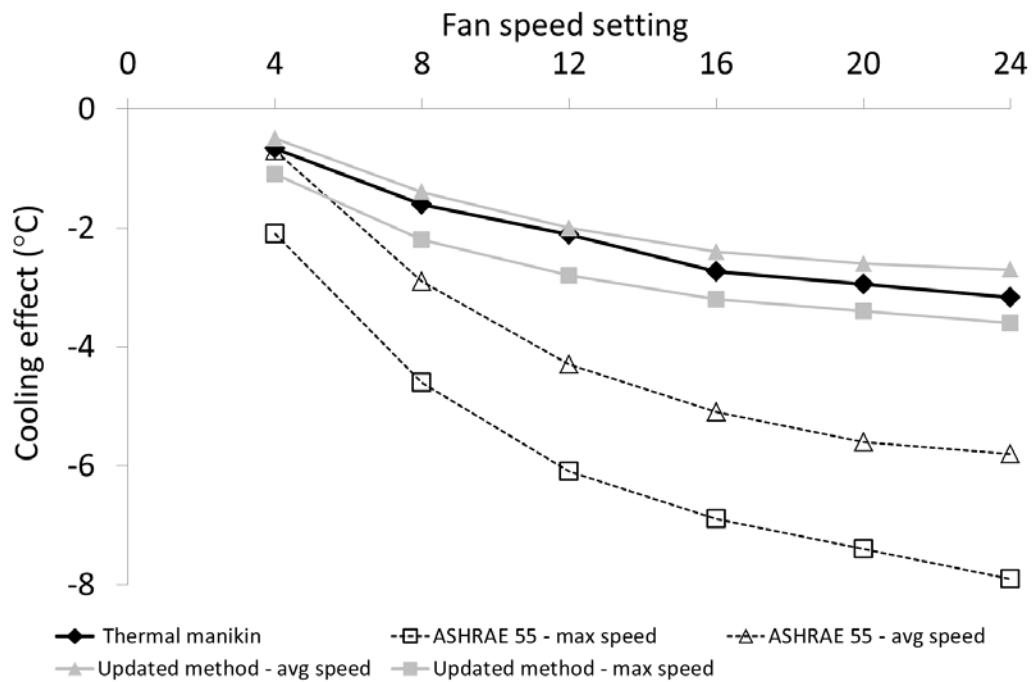
#### *4.2. Updated standard effective temperature method for assessing the cooling effect*

Fig. 10 shows substantial differences between the cooling effect obtained with the manikin and the one obtained using the approach of ASHRAE Standard 55-2013. One possible explanation is related to the way that the cooling effect is calculated in ASHRAE Standard 55-2013. In the standard, the entire effect of elevated air speed on SET\* is assigned only to the reduction of dry-bulb temperature. In actual implementation, the mean radiant temperature is kept constant. For example, Fig. 10 was obtained with a dry-bulb temperature equal to the radiant temperature at 26 °C. For a fan-speed setting of 16 ( $P = 11.2$  W), and utilizing the average airspeed option, the cooling effect would be 5.1 °C. According to the assessment method in Standard 55-2013, the actual environment (dry bulb temperature = mean radiant temperature = 26 °C, airspeed = 0.94 m/s) is thermally equivalent to a space with a dry bulb temperature of 20.9 °C, a mean radiant temperature of 26 °C, and an airspeed of 0.15 m/s (equivalent to “still air” as specified in the standard). In commercial air-conditioned buildings, one would not commonly find in such a large difference between the dry-bulb and mean radiant temperatures. Consequently, the assessed cooling effect is

misleadingly large; in an air-conditioned space, one would expect a much smaller difference between the dry-bulb and mean radiant temperatures.

An updated calculation method can be considered. In this updated method, the mean radiant temperature is assumed to be equal to the dry-bulb temperature and the effect of elevated air speed is assigned to reducing both temperature metrics. To assess the performance of this updated method, it was applied to the data from the present study, and the results are plotted in Fig. 10. We find that the results from the calculation are now much closer to the measurements performed with the thermal manikin. For example, if the fan speed setting is 16 ( $P = 11.2$  W) and the average airspeed option is used, then the cooling effect would be equal to 2.4 °C. The actual environment (dry bulb temperature = mean radiant temperature = 26 °C, airspeed = 0.94 m/s) is thermally equivalent to a space with dry bulb temperature = mean radiant temperature = 23.6 °C and airspeed = 0.15 m/s (i.e., nominally still air).

To assess which method for SET\* implementation and which air speed measurements should be used, experiments with human subjects are needed. At this stage, we can only suggest that the updated method shows promise for providing more realistic and therefore more practically useful results.



**Fig. 10.** Comparison of cooling effects measured by thermal manikin, calculated according to ASHRAE Standard 55-2013, and calculated using an updated method that considers changes in both the dry-bulb and mean radiant temperature. See Table A in the Supplemental Information for the relationships among fan speed setting, fan power, and air speed.

## 5. Conclusions

The performance of a brushless DC stand fan was evaluated in experiments that measured manikin-based equivalent temperature, fan power consumption and cooling fan efficiency (CFE) index at four different dry-bulb temperatures, six fan speed settings, two fan-manikin distances and two fan-manikin orientations.

The measured median values (interquartile ranges) were as follows: for whole-body cooling effect  $-2.4\text{ }^{\circ}\text{C}$  ( $-3.7\text{ }^{\circ}\text{C}$ ,  $-1.5\text{ }^{\circ}\text{C}$ ), for fan power  $9.2\text{ W}$  ( $4.7\text{ W}$ ,  $13.9\text{ W}$ ), and for the CFE index  $0.27\text{ }^{\circ}\text{C/W}$  ( $0.19\text{ }^{\circ}\text{C/W}$ ,  $0.41\text{ }^{\circ}\text{C/W}$ ). The results showed that the whole-body cooling effect and the CFE index are influenced by dry-bulb temperature, fan speed setting,

and fan-manikin distance but not by fan-manikin orientation. With the tested stand fan, the cooling effect is homogenous across the upper body owing to the wide airflow field generated by the stand fan. With lower air temperatures and for the shorter fan-manikin distance, the cooling effect and CFE are enhanced. However, increasing fan speed setting enhances simultaneously the whole-body cooling effect and also fan power use. Consequently, the CFE index exhibits a non-monotonic relationship with fan speed setting and the peak value is attained for an intermediate air speed setting of 8 at which the fan-power consumption was 4.7 W and the airspeed at height of the fan axis was 1.1 m/s at 1 m and 0.5 m/s at 2 m from the fan.

Cooling effects, calculated according to ASHRAE Standard 55-2013 based on maximum speed and average speed, were compared with thermal manikin measured results and substantial differences were found. An updated calculation method is proposed, which apportions the cooling effect caused by elevated air movement to reductions in both the dry-bulb and mean radiant temperatures. The results of this updated method are much closer to the measurements performed with the thermal manikin than are the results using methods prescribed in Standard 55-2013. Future experiments using human subjects would be warranted to pursue this matter more completely, since the manikin tests here did not include the effects of latent cooling.

As compared with previous test results for an AC stand fan, the CFE index of the brushless DC fan is approximately three times better, primarily because of the better energy efficiency of the DC fan.

Standard testing methods and standardized evaluation metrics such as the CFE index are necessary for mechanical system designers, fan manufacturers, policy makers, and users. Experiments with human subjects, incorporating human perception, acceptability and

preference for fan generated non-uniform airflow field accompanied by thermal environment with elevated dry-bulb temperature, would be necessary for further evaluation.

### **Acknowledgements**

This research was funded in part by the Republic of Singapore's National Research Foundation through a grant to the Berkeley Education Alliance for Research in Singapore (BEARS) for the Singapore-Berkeley Building Efficiency and Sustainability in the Tropics (SinBerBEST) Program. BEARS has been established by the University of California, Berkeley as a center for intellectual excellence in research and education in Singapore. Acknowledgement is also given to Department of Building, National University of Singapore, for supplying experimental facilities.

### **References**

- [1] Thorshauge J. Air-velocity fluctuation in the occupied zone of ventilated spaces. *ASHRAE Trans* 1982; 88(2): 753-64.
- [2] Rohles FH, Konz SA, Jones BW. Ceiling fans as extenders of the summer comfort envelope. *ASHRAE Trans* 1983; 89(1): 245-63.
- [3] Scheatzle DG, Wu H, Yellot J. Extending the summer comfort envelope with ceiling fans in hot, arid climates. *ASHRAE Trans* 1989; 95(1): 269-80.
- [4] Bauman FS, Zhang H, Arens EA, Benton CC. Localized comfort control with a desktop task conditioning system: Laboratory and field measurements. *ASHRAE Trans* 1993; 99(2): 733-49.
- [5] Bauman FS, Carter TG, Baughman AV, Arens EA. Field study of the impact of a desktop task/ambient conditioning system in office buildings. *ASHRAE Trans* 1998; 104(1): 1-19.
- [6] Zhang H, Arens E, Kim D, Buchberger E, Bauman F, Huizenga C. Comfort, perceived air quality, and work performance in a low-power task-ambient conditioning system. *Build Environ* 2010; 45: 29-39.
- [7] Sekhar SC. Higher space temperatures and better thermal comfort — a tropical analysis. *Energy Build* 1995; 23: 63-70.
- [8] Aynsley R. Saving energy with indoor air movement. *Int J Vent* 2005; 4: 167-76.
- [9] Schiavon S, Melikov AK. Energy saving and improved comfort by increased air movement. *Energy Build* 2008; 40: 1954-60.
- [10] Fanger PO, Christensen NK. Perception of draught in ventilated spaces. *Ergonomics* 1986; 29: 215-35.

- [11] McIntyre DA. Preferred air speeds for comfort in warm conditions. *ASHRAE Trans* 1978; 84(2): 264-77.
- [12] Tanabe S-I, Kimura K-I. Effects of air temperature, humidity and air movement on thermal comfort under hot and humid conditions. *ASHRAE Trans* 1994; 100(2): 953-69.
- [13] Fountain M, Arens E, de Dear R, Bauman F, Miura K. Locally controlled air movement preferred in warm isothermal environments. *ASHRAE Trans* 1994; 100(2): 937-52.
- [14] Chow WK, Fung WY. Investigation of the subjective response to elevated air velocities: climate chamber experiments in Hong Kong. *Energy Build* 1994; 20: 187-92.
- [15] Arens E, Xu T, Miura K, Zhang H, Fountain M, Bauman F. A study of occupant cooling by personally controlled air movement. *Energy Build* 1998; 27: 45-59.
- [16] Khedari J, Yamtraipat N, Pratintong N, Hirunlabh J. Thailand ventilation comfort chart. *Energy Build* 2000; 32: 245-49.
- [17] Ho SH, Rosario L, Rahman MM. Thermal comfort enhancement by using a ceiling fan. *Appl Therm Eng* 2009; 29: 1648-56.
- [18] Candido C, de Dear RJ, Lamberts R, Bittencourt L. Air movement acceptability limits and thermal comfort in Brazil's hot humid climate zone. *Build Environ* 2010; 45: 222-9.
- [19] Zhai Y, Zhang H, Zhang Y, Pasut W, Arens E, Meng Q. Comfort under personally controlled air movement in warm and humid environments. *Build Environ* 2013; 65: 109-17.
- [20] Sekhar SC, Gong N, Tham KW, Cheong KW, Melikov AK, Wyon DP, Fanger PO. Findings of personalized ventilation studies in a hot and humid climate. *HVAC&R Res* 2005; 11: 603-20.
- [21] de Dear RJ, Akimoto T, Arens EA, Brager G, Candido C, Cheong KWD, Li B, Nishihara N, Sekhar SC, Tanabe S, Toftum J, Zhang H, Zhu Y. Progress in thermal comfort research over the last twenty years. *Indoor Air* 2013; 23: 442-61.
- [22] ANSI/ASHRAE (2013). Thermal environmental conditions for human occupancy. Atlanta. GA, American Society of Heating, refrigeration and Air-Conditioning Engineers (ANSI/ASHRAE standard 55-2013).
- [23] CEN (2007). EN 15251-2007, Criteria for the indoor environment including thermal, indoor air quality, light and noise. Brussels, European committee for Standardization.
- [24] ISO 7730 (2005). Moderate thermal environment-determination of the PMV and PPD indices and specification of the conditions for thermal comfort. Geneva, International Organization for Standardization.
- [25] Fang L, Wyon DP, Clausen G, Fanger PO. Impact of indoor air temperature and humidity in an office on perceived air quality, SBS symptoms and performance. *Indoor Air* 2004; 14 (Suppl. 7): 74-81.
- [26] Melikov AK, Kaczmarczyk J. Air movement and perceived air quality. *Build Environ* 2012; 47: 400-409.
- [27] Skwarczynski MA, Melikov AK, Kaczmarczyk J, Lyubenova V. Impact of individually controlled facially applied air movement on perceived air quality at high humidity. *Build Environ* 2010; 45: 2170-6.
- [28] Zhang H, Arens E, Pasut W. Air temperature thresholds for indoor comfort and perceived air quality. *Build Res Inf* 2011; 39: 134-44.

- [29] Pasut W, Arens E, Zhang H, Zhai Y. Enabling energy-efficient approaches to thermal comfort using room air motion. *Build Environ* 2014; 79: 13-19.
- [30] Schiavon S, Melikov AK. Introduction of a cooling-fan efficiency index. *HVAC&R Res* 2009; 15: 1121-44.
- [31] Schmidt K, Patterson DJ. Performance results for a high efficiency tropical ceiling fan and comparisons with conventional fans: Demand side management via small appliance efficiency. *Renew Energy* 2001; 22: 169-76.
- [32] Liu CS, Hwang JC, Chen LR, Fu CC. Development of new structure of brushless DC servo motor for ceiling fan. In: *Proceedings of 4th IEEE Conference on Industrial Electronics and Applications* 2009; Xi'an, China, 2640-3.
- [33] Umans SD. *Fitzgerald & Kingsley's Electric Machinery* (Seventh edition), McGraw-Hill Series in Electrical Engineering, 2013.
- [34] JCGM 100 (2008). *Evaluation of measurement data-Guide to the expression of uncertainty in measurement (GUM)*. Paris, International Bureau of Weights and Measures.
- [35] JCGM 104 (2009). *Evaluation of measurement data-An introduction to the "Guide to the expression of uncertainty in measurement" and related documents*. Paris, International Bureau of Weights and Measures.
- [36] de Dear RJ, Leow KG, Foo SC. Thermal comfort in the humid tropics: Field experiments in air conditioned and naturally ventilated buildings in Singapore. *Int J Biometeorol* 1991; 34: 259-65.
- [37] Melikov A. Breathing thermal manikins for indoor environment assessment: important characteristics and requirements. *Eur J Appl Physiol* 2004; 92: 710-13.
- [38] Holmér I. Thermal manikin history and applications. *Eur J Appl Physiol* 2004; 92: 614-18.
- [39] Anttonen H, Niskanen J, Meinander H, Bartels V, Kuklane K, Reinertsen RE, Varietas S, Soltynski K. Thermal manikin measurements — Exact or not? *Int J Occup Saf Ergo* 2004; 10: 291-300.
- [40] Tanabe S, Arens EA, Bauman FS, Zhang H, Madsen TL. Evaluating thermal environments by using a thermal manikin with controlled skin surface temperature. *ASHRAE Trans* 1994; 100(1): 39-48.
- [41] Melikov AK, Cermak R, Majer M. Personalized ventilation: Evaluation of different air terminal devices. *Energy Build* 2002; 34: 829-36.
- [42] Yang B, Melikov A, Sekhar C. Performance evaluation of ceiling mounted personalized ventilation system. *ASHRAE Trans* 2009; 115(2): 395-406.
- [43] Huang L, Ouyang Q, Zhu Y, Jiang L. A study about the demand for air movement in warm environment. *Build Environ* 2013; 61: 27-33.
- [44] Schiavon S, Hoyt T, Piccioli A. Web application for thermal comfort visualization and calculation according to ASHRAE Standard 55. *Build Simul* 2014, 7: 321-34.
- [45] ASHRAE (2013). *ASHRAE Handbook-Fundamentals*. Atlanta, GA, American Society of Heating, refrigeration and Air-Conditioning Engineers.
- [46] Gagge AP, Stolwijk JAJ, Nishi Y. An effective temperature scale based on a simple model of human physiological regulatory response. *ASHRAE Trans* 1971; 77(1): 247-62.



[47] Hoyt T, Schiavon S, Piccioli A, Moon D, and Steinfeld K. 2013. CBE Thermal Comfort Tool. Center for the Built Environment, University of California Berkeley, <http://cbe.berkeley.edu/comforttool>

**SUPPLEMENTAL INFORMATION**

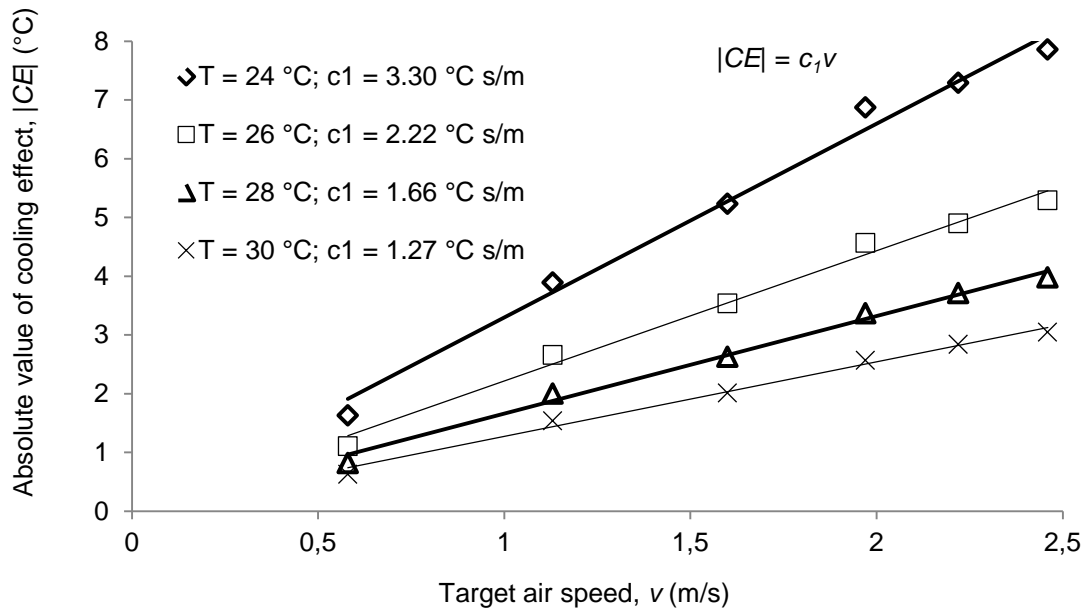


**Fig. A1.** Cooling effect versus target air speed for 1 m fan-manikin distance and front fan-manikin orientation.

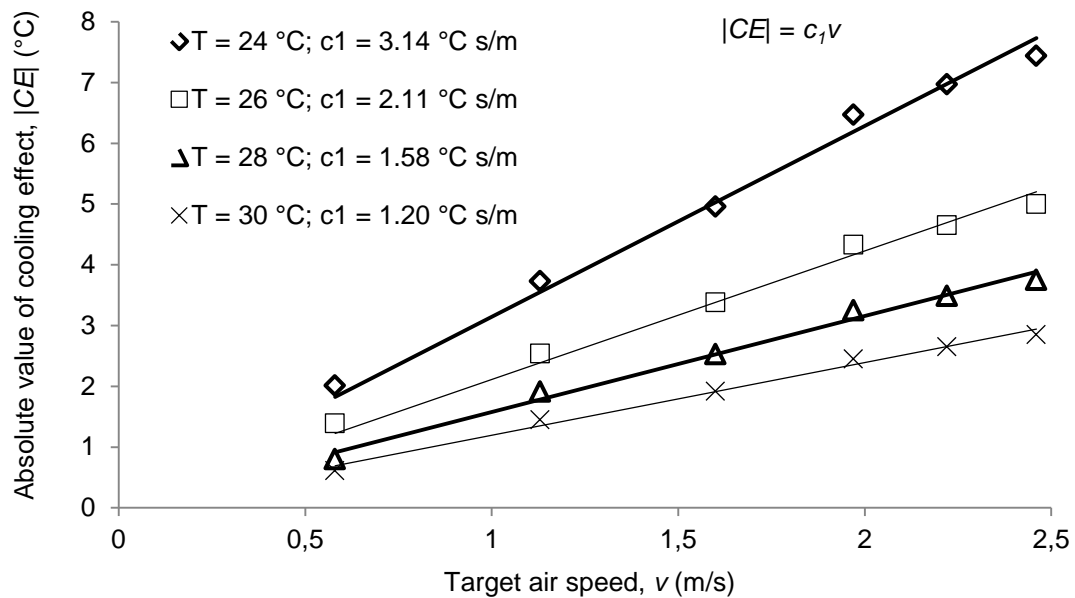


**Fig. A2.** Cooling effect versus target air speed for 1 m fan-manikin distance and side fan-manikin orientation.

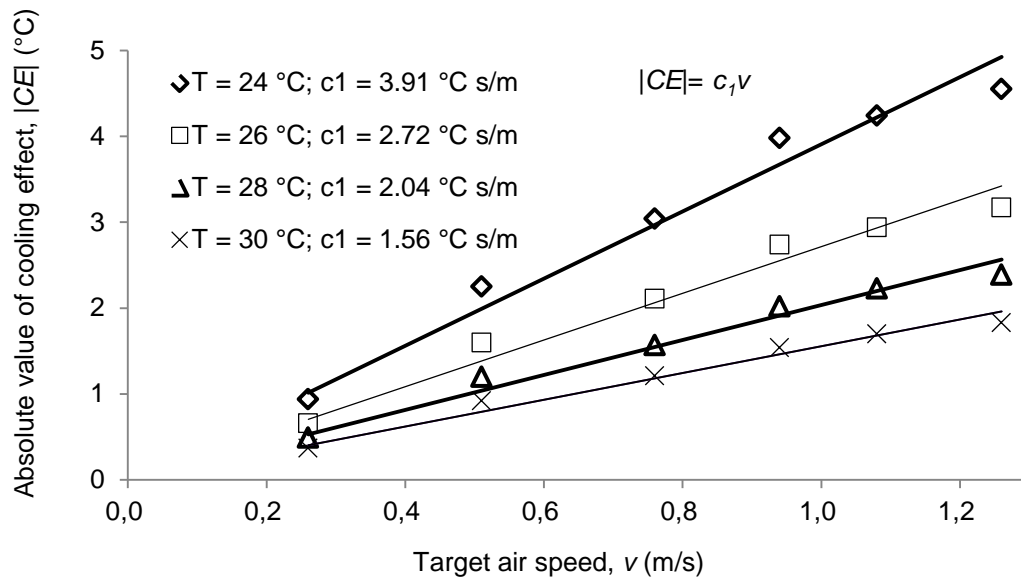


**Fig. A3.** Cooling effect versus target air speed for 2 m fan-manikin distance and front fan-manikin orientation.

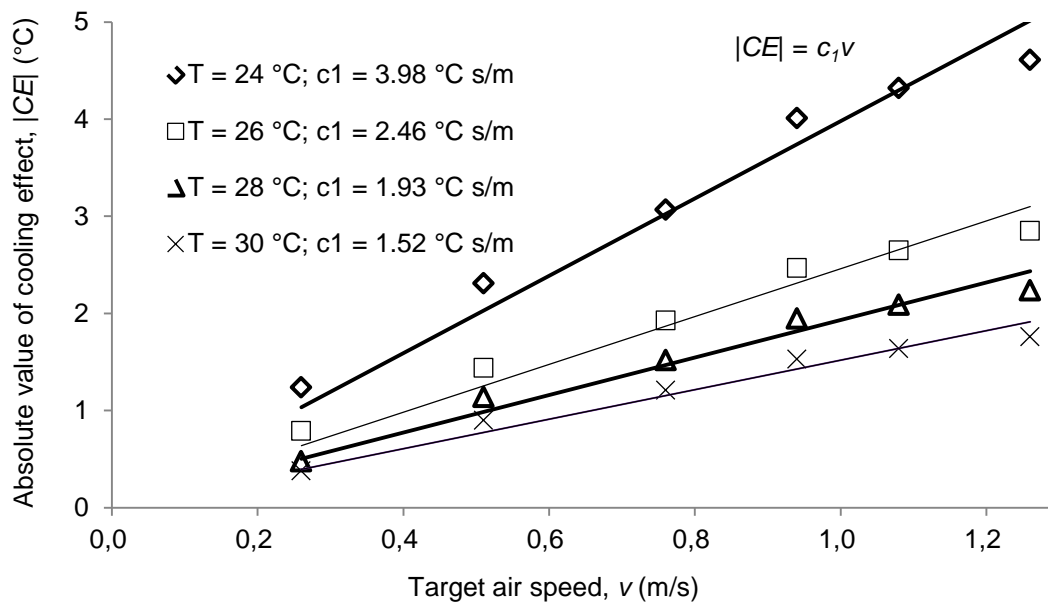


**Fig. A4.** Cooling effect versus target air speed for 2 m fan-manikin distance and side fan-manikin orientation.

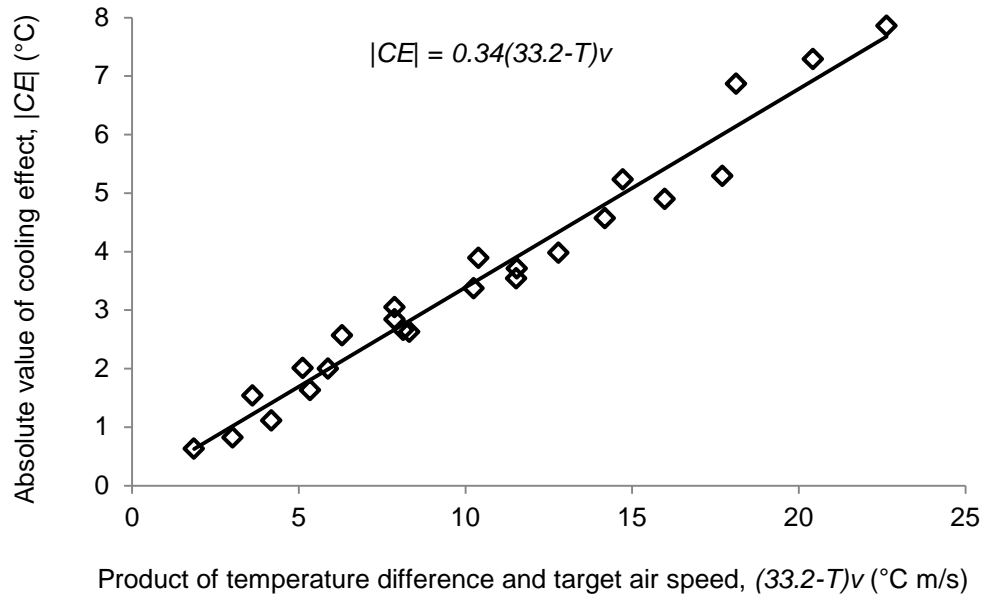


**Fig. B1.** Cooling effect versus product of temperature difference and target air speed for 1 m fan-manikin distance and front fan-manikin orientation.

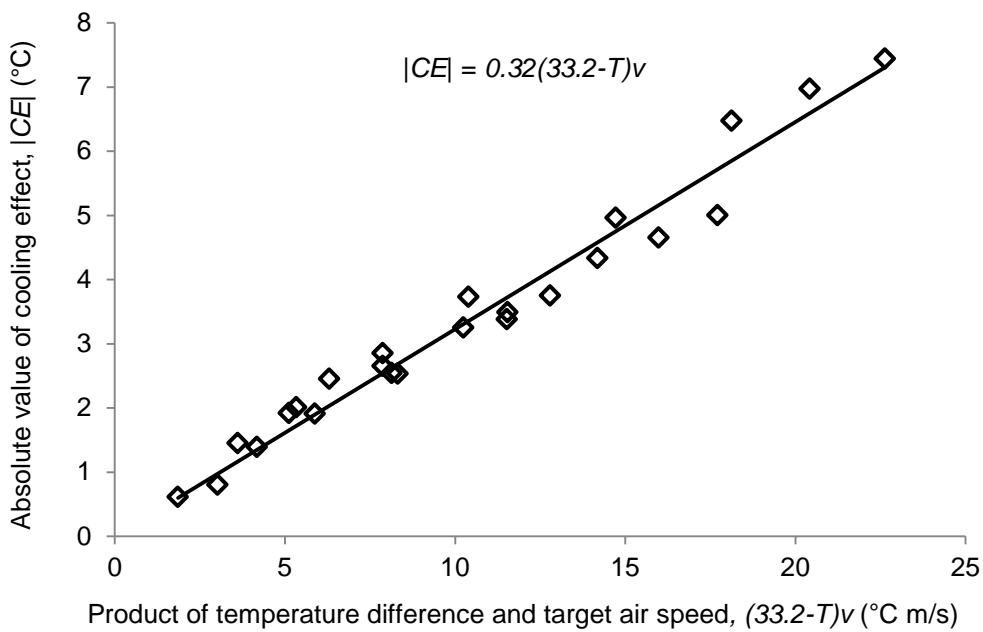


**Fig. B2.** Cooling effect versus product of temperature difference and target air speed for 1 m fan-manikin distance and side fan-manikin orientation.

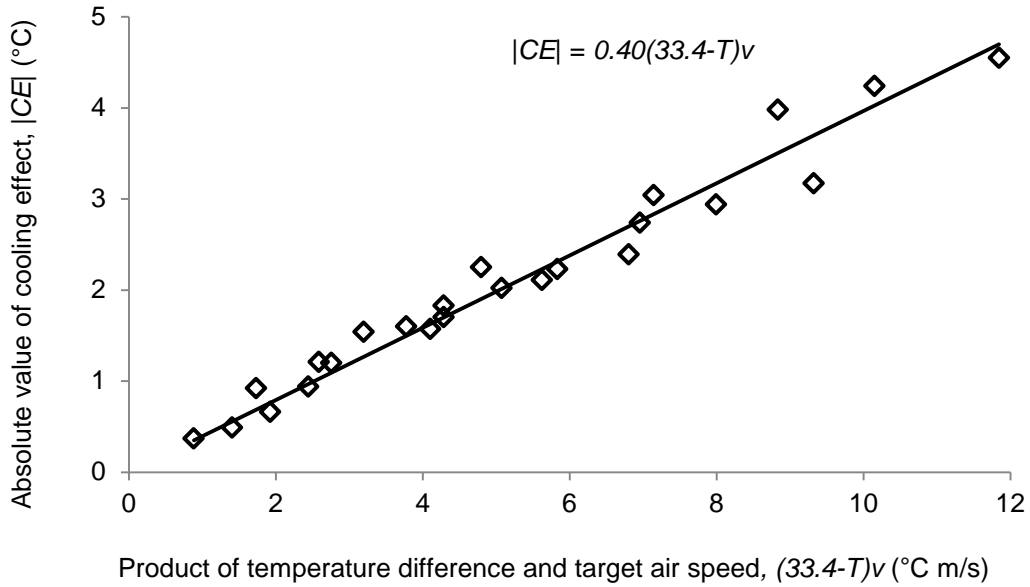


**Fig. B3.** Cooling effect versus product of temperature difference and target air speed for 2 m fan-manikin distance and front fan-manikin orientation.

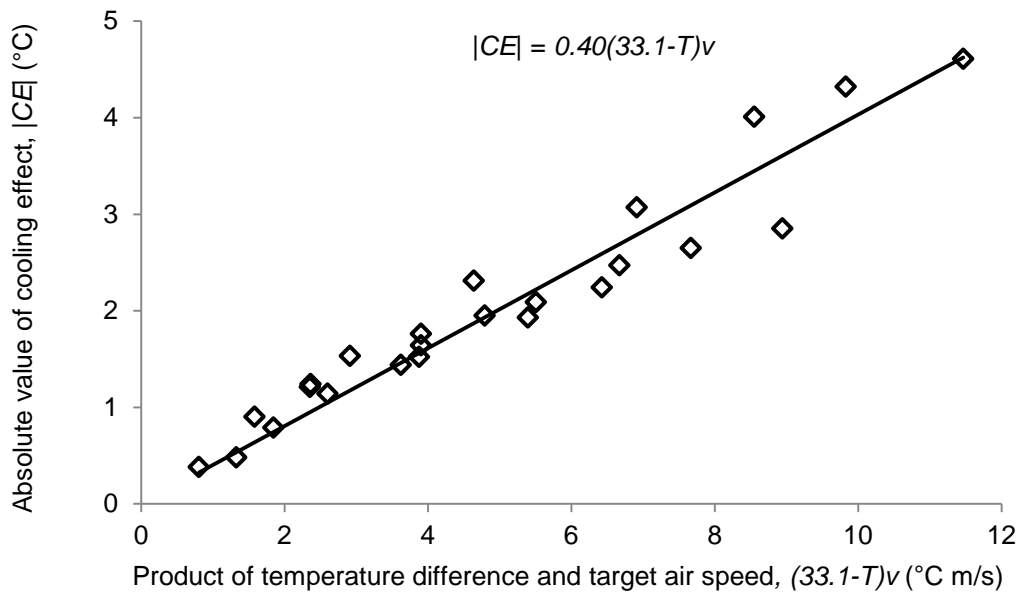


**Fig. B4.** Cooling effect versus product of temperature difference and target air speed for 2 m fan-manikin distance and side fan-manikin orientation.

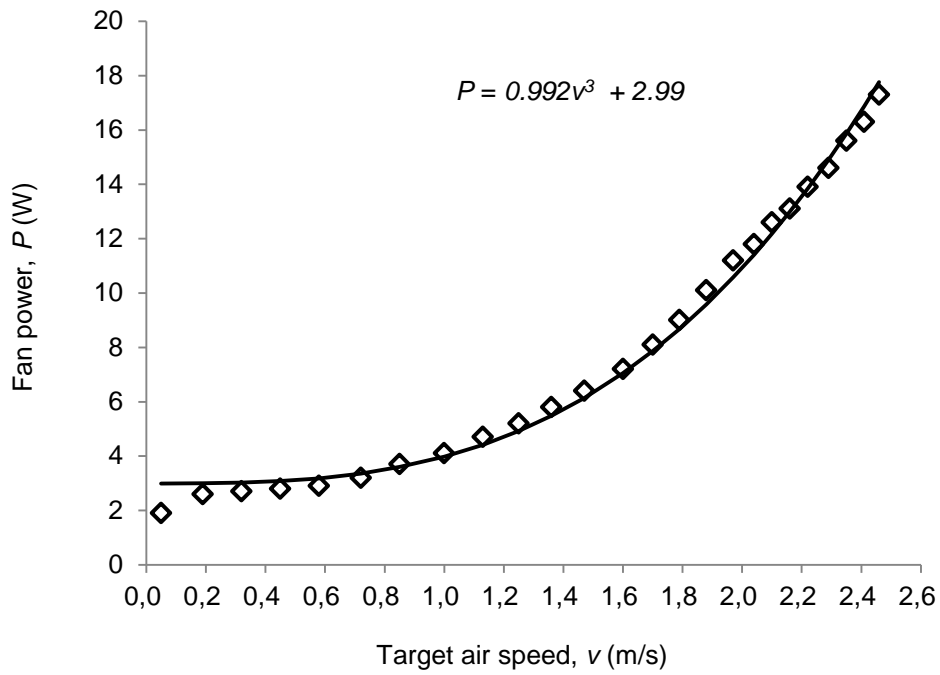


**Fig. C1.** Fan power versus target air speed for 1 m fan-manikin distance.

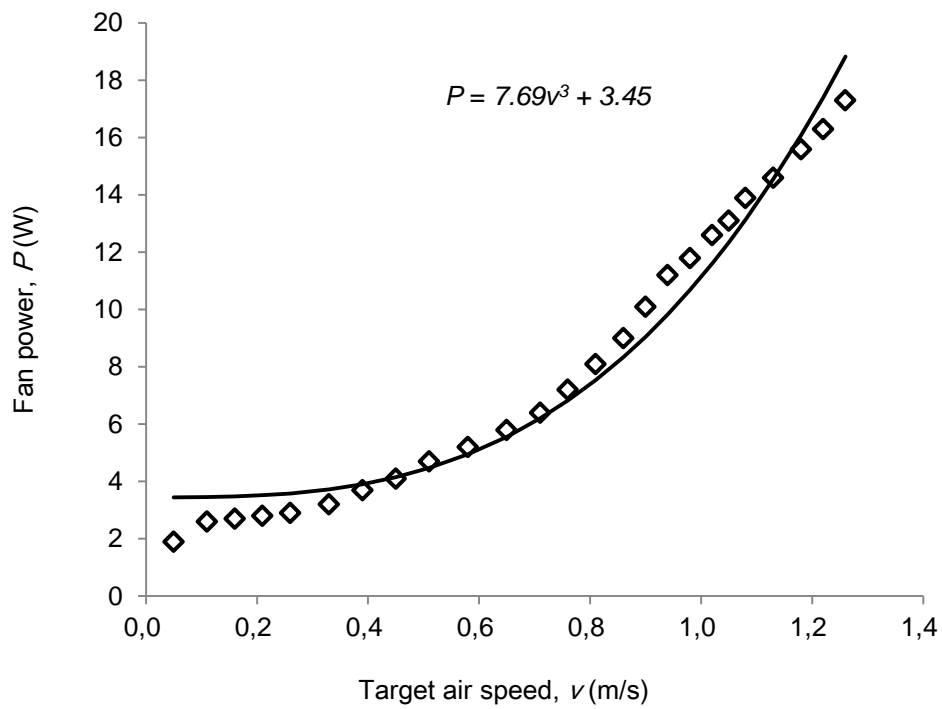


**Fig. C2.** Fan power versus target air speed for 2 m fan-manikin distance.

**Table A.** Fan speed settings, fan power and air speeds measured at 1.1 m height (same as height of fan blade center) at the target location for the two tested distances between the fan and the target location (1 and 2 m).

Fan speed setting	Fan power (W)	Target point air speed (m/s)	
		1 m distance	2 m distance
1	2.6	0.19	0.11
2	2.7	0.32	0.16
3	2.8	0.45	0.21
4	2.9	0.58	0.26
5	3.2	0.72	0.33
6	3.7	0.85	0.39
7	4.1	1.00	0.45
8	4.7	1.13	0.51
9	5.2	1.25	0.58
10	5.8	1.36	0.65
11	6.4	1.47	0.71
12	7.2	1.60	0.76
13	8.1	1.70	0.81
14	9.0	1.79	0.86
15	10.1	1.88	0.90
16	11.2	1.97	0.94
17	11.8	2.04	0.98
18	12.6	2.10	1.02
19	13.1	2.16	1.05
20	13.9	2.22	1.08
21	14.6	2.29	1.13
22	15.6	2.35	1.18
23	16.3	2.41	1.22
24	17.3	2.46	1.26

**Table B.** Sample uncertainty ( $U$ ) and uncertainty of a derived quality ( $U_c$ ) with 95% confidence level. <sup>a</sup>

Quantity	$U_{\text{meas}}$	$U_{\text{instr}}$	$U$	$U_c$
manikin based				$\Delta t_{eq}$ : 0.3 °C
equivalent temperature, $t_{eq}$	<0.05 °C	0.2 °C	0.21 °C	CFE: 0.009 °C/W
Fan power, $P$	0.1 W	0.5 W	0.51 W	CFE: 0.009 °C/W
Air speed	See footnote b			
Air temperature	See footnote c			
Relative humidity	See footnote d			

<sup>a</sup> Sample standard uncertainty ( $U$ ) was calculated as the combination of maximum uncertainty of measurement ( $U_{\text{meas}}$ ) and inherent uncertainty of the instrument ( $U_{\text{instr}}$ ).

<sup>b</sup> 0.01 m/s  $\pm$ 1% of readings for velocity.

<sup>c</sup>  $\pm$ 0.4 °C of readings for temperature range from 0-60 °C.

<sup>d</sup>  $\pm$ 3% of readings for relative humidity range from 5-95%.



**Table C.** Whole-body cooling effect, fan power and cooling fan efficiency (CFE) index for four dry-bulb temperatures (24, 26, 28 and 30 °C), six fan speed settings (4, 8, 12, 16, 20 and 24), two orientations (front and side) and two fan-manikin distances (1 and 2 m).

Fan-Manikin distance, m	Orientation	Fan speed setting	Dry-bulb temperature °C	Whole- body cooling effect ( $\Delta t_{eq}$ ) °C	Fan power W	CFE °C/W
1	Front	4	24	-1.6	2.9	0.56
1	Front	8	24	-3.9	4.7	0.83
1	Front	12	24	-5.2	7.2	0.73
1	Front	16	24	-6.9	11.2	0.61
1	Front	20	24	-7.3	13.9	0.52
1	Front	24	24	-7.9	17.3	0.45
1	Front	4	26	-1.1	2.9	0.38
1	Front	8	26	-2.7	4.7	0.57
1	Front	12	26	-3.5	7.2	0.49
1	Front	16	26	-4.6	11.2	0.41
1	Front	20	26	-4.9	13.9	0.35
1	Front	24	26	-5.3	17.3	0.31
1	Front	4	28	-0.8	2.9	0.28
1	Front	8	28	-2.0	4.7	0.43
1	Front	12	28	-2.6	7.2	0.37
1	Front	16	28	-3.4	11.2	0.30
1	Front	20	28	-3.7	13.9	0.27
1	Front	24	28	-4.0	17.3	0.23
1	Front	4	30	-0.6	2.9	0.22
1	Front	8	30	-1.5	4.7	0.33
1	Front	12	30	-2.0	7.2	0.28
1	Front	16	30	-2.6	11.2	0.23
1	Front	20	30	-2.8	13.9	0.20
1	Front	24	30	-3.1	17.3	0.18
1	Side	4	24	-2.0	2.9	0.69
1	Side	8	24	-3.7	4.7	0.79
1	Side	12	24	-5.0	7.2	0.69
1	Side	16	24	-6.5	11.2	0.58
1	Side	20	24	-7.0	13.9	0.50
1	Side	24	24	-7.4	17.3	0.43
1	Side	4	26	-1.4	2.9	0.48
1	Side	8	26	-2.5	4.7	0.54
1	Side	12	26	-3.4	7.2	0.47
1	Side	16	26	-4.3	11.2	0.39
1	Side	20	26	-4.7	13.9	0.33
1	Side	24	26	-5.0	17.3	0.29
1	Side	4	28	-0.8	2.9	0.28
1	Side	8	28	-1.9	4.7	0.41
1	Side	12	28	-2.5	7.2	0.35
1	Side	16	28	-3.3	11.2	0.29
1	Side	20	28	-3.5	13.9	0.25
1	Side	24	28	-3.8	17.3	0.22

1	Side	4	30	-0.6	2.9	0.21
1	Side	8	30	-1.5	4.7	0.31
1	Side	12	30	-1.9	7.2	0.27
1	Side	16	30	-2.5	11.2	0.22
1	Side	20	30	-2.7	13.9	0.19
1	Side	24	30	-2.9	17.3	0.16
2	Front	4	24	-0.9	2.9	0.32
2	Front	8	24	-2.3	4.7	0.48
2	Front	12	24	-3.0	7.2	0.42
2	Front	16	24	-4.0	11.2	0.36
2	Front	20	24	-4.2	13.9	0.31
2	Front	24	24	-4.6	17.3	0.26
2	Front	4	26	-0.7	2.9	0.23
2	Front	8	26	-1.6	4.7	0.34
2	Front	12	26	-2.1	7.2	0.29
2	Front	16	26	-2.7	11.2	0.24
2	Front	20	26	-2.9	13.9	0.21
2	Front	24	26	-3.2	17.3	0.18
2	Front	4	28	-0.5	2.9	0.17
2	Front	8	28	-1.2	4.7	0.26
2	Front	12	28	-1.6	7.2	0.22
2	Front	16	28	-2.0	11.2	0.18
2	Front	20	28	-2.2	13.9	0.16
2	Front	24	28	-2.4	17.3	0.14
2	Front	4	30	-0.4	2.9	0.13
2	Front	8	30	-0.9	4.7	0.20
2	Front	12	30	-1.2	7.2	0.17
2	Front	16	30	-1.5	11.2	0.14
2	Front	20	30	-1.7	13.9	0.12
2	Front	24	30	-1.8	17.3	0.11
2	Side	4	24	-1.2	2.9	0.43
2	Side	8	24	-2.3	4.7	0.49
2	Side	12	24	-3.1	7.2	0.43
2	Side	16	24	-4.0	11.2	0.36
2	Side	20	24	-4.3	13.9	0.31
2	Side	24	24	-4.6	17.3	0.27
2	Side	4	26	-0.8	2.9	0.27
2	Side	8	26	-1.4	4.7	0.31
2	Side	12	26	-1.9	7.2	0.27
2	Side	16	26	-2.5	11.2	0.22
2	Side	20	26	-2.7	13.9	0.19
2	Side	24	26	-2.9	17.3	0.16
2	Side	4	28	-0.5	2.9	0.17
2	Side	8	28	-1.1	4.7	0.24
2	Side	12	28	-1.5	7.2	0.21
2	Side	16	28	-2.0	11.2	0.17
2	Side	20	28	-2.1	13.9	0.15
2	Side	24	28	-2.2	17.3	0.13
2	Side	4	30	-0.4	2.9	0.13
2	Side	8	30	-0.9	4.7	0.19

2	Side	12	30	-1.2	7.2	0.17
2	Side	16	30	-1.5	11.2	0.14
2	Side	20	30	-1.6	13.9	0.12
2	Side	24	30	-1.8	17.3	0.10

**Table D.** Best-fit parameters  $c^*$  and  $T^*$  for different fan-manikin distances and orientations.

Distance (m)	Orientation	$c^*$ (s/m)	$T^*$ (°C)	$R^2$
1	Front	0.34	33.2	0.97
1	Side	0.32	33.2	0.97
2	Front	0.40	33.4	0.96
2	Side	0.40	33.1	0.93

**Table E.** SET\* calculated for a dry-bulb temperature of 26 °C.

Measuring height (m)	Fan speed setting	Air speed (m/s)	SET* °C	Cooling effect calculated with SET* °C	Cooling effect measured by thermal manikin °C
0.1	4	0.10	26.5		
0.6	4	0.19	25.8	-1.0	
1.1	4	0.26	25.2	-2.1	
1.7	4	0.08	26.5		
Average <sup>a</sup>		0.18	25.9	-0.7	-0.7
0.1	8	0.09	26.5		
0.6	8	0.36	24.7	-3.3	
1.1	8	0.51	24.1	-4.6	
1.7	8	0.08	26.5		
Average <sup>a</sup>		0.32	24.9	-2.9	-1.6
0.1	12	0.08	26.5		
0.6	12	0.54	24.0	-4.9	
1.1	12	0.76	23.5	-6.1	
1.7	12	0.08	26.5		
Average <sup>a</sup>		0.46	24.3	-4.3	-2.1
0.1	16	0.08	26.5		
0.6	16	0.68	23.7	-5.7	
1.1	16	0.94	23.1	-6.9	
1.7	16	0.09	26.5		
Average <sup>a</sup>		0.57	23.9	-5.1	-2.7
-0.1	20	0.07	26.5		
0.6	20	0.81	23.4	-6.4	
1.1	20	1.08	22.9	-7.4	
1.7	20	0.10	26.5		
Average <sup>a</sup>		0.65	23.7	-5.6	-2.9
0.1	24	0.07	26.5		
0.6	24	0.75	23.5	-6.1	
1.1	24	1.26	22.7	-7.9	
1.7	24	0.15	26.3		
Average <sup>a</sup>		0.69	23.6	-5.8	-3.2

<sup>a</sup> The average air speed is average of measurements at 0.1, 0.6, and 1.1 m.